Chemo-optogenetics

Tunable and Photoswitchable Chemically Induced Dimerization for Chemo-optogenetic Control of Protein and Organelle Positioning

Xi Chen and Yao-Wen Wu*

Abstract: *The spatiotemporal dynamics of proteins and organelles play an important role in controlling diverse cellular processes. Optogenetic tools using photosensitive proteins and chemically induced dimerization (CID), which allow control of protein dimerization, have been used to elucidate the dynamics of biological systems and to dissect the complicated biological regulatory networks. However, the inherent limitations of current optogenetic and CID systems remain a significant challenge for the fine-tuning of cellular activity at precise times and locations. Herein, we present a novel chemo-optogenetic approach, photoswitchable chemically induced dimerization (psCID), for controlling cellular function by using blue light in a rapid and reversible manner. Moreover, psCID is tunable; that is, the dimerization and dedimerization degrees can be fine-tuned by applying different doses of illumination. Using this approach, we control the localization of proteins and positioning of organelles in live cells with high spatial (µm) and temporal (ms) precision.*

Cellular processes are often controlled by the dynamic distribution of molecules or organelles that are organized in space and time. To unravel the complex and dynamic nature of the underlying biological systems, acute and tunable perturbations with high spatial and temporal resolution are required. Chemical and optogenetic tools that can modulate protein activity in cells are robust approaches for controlling protein function and perturbing associated biological processes.[1] However, many optogenetic approaches using photosensitive proteins suffer from several problems in tunability, dynamic range, and turn-off speed.[1c,d, 2]

[*] Dr. X. Chen, Prof. Dr. Y.-W. Wu
Chemical Genomics Centre of the Max Planck Society
Otto-Hahn-Str. 15, 44227 Dortmund (Germany)
and
Max Planck Institute of Molecular Physiology
Otto-Hahn-Str. 11, 44227 Dortmund (Germany)
E-mail: yaowen.wu@mpi-dortmund.mpg.de

Dr. X. Chen, Prof. Dr. Y.-W. Wu
Department of Chemistry, Umeå University
90187 Umeå (Sweden)
E-mail: yaowen.wu@umu.se

Supporting information and the ORCID identification number(s) for the author(s) of this article can be found under:
https://doi.org/10.1002/anie.201800140.

Chemically induced dimerization (CID) is a powerful tool for modulating protein function by bringing two proteins in close proximity of each other. The induced binding is quite stable (K_d in the nanomolar range) without addition of competitor compounds, in comparison to the relatively low binding affinity of photoreceptors (K_d usually in the micromolar range). However, although CID can be manipulated reversibly, its temporal resolution is restricted by the time required for cell permeation and its spatial precision is limited by the free diffusion of the dimerizer throughout the cell.[3] The temporal resolution is improved by using photocaged dimerizers,[1b] such as caged rapamycin.[4] Photocleavable MeNV-HaXS,[5] caged TMP-HTag,[6] and NvocTMP-Cl[7] are restrained from free diffusion through covalent binding to the dimerization module. However, in contrast to optogenetic systems using photosensitive proteins, the chemical dimerizers cannot be turned on and off by light. Therefore, a photoswitchable CID would be a valuable light-induced dimerization approach for a wide range of biological studies. In this work, we present an acute, tunable, and photoswitchable chemically induced dimerization (psCID), which enables the activity of proteins to be switched on and off by light.
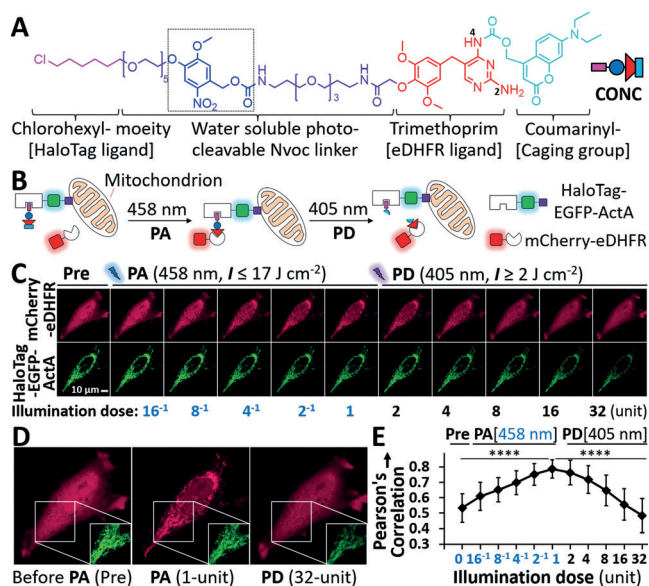
Transport of various intracellular cargos (for example, proteins and organelles) along cytoskeleton filaments is essential for the morphogenesis and function in eukaryotic cells.[8] The positioning of organelles locally orchestrates many cellular processes including cell signaling, cell polarization, and neurite outgrowth.[9] Retrograde transport of cargos along microtubules toward the cell center is typically mediated by cytoplasmic dynein and dynactin, and requires the evolutionarily conserved motor adaptor Bicaudal D (BicD).[10] In this work, we use the psCID system to rapidly activate and deactivate dynein-mediated endosome transport with light, thereby manipulating endosome positioning within a living cell.

Based on a modular design, we synthesized the photoswitchable chemical dimerizer, 4-coumarin-TMP-Nvoc-Cl (CONC; Supporting Information, Scheme S1). CONC features a chlorohexyl moiety for covalent binding to a bacterial alkyldehalogenase mutant (HaloTag), a trimethoprim (TMP) moiety for noncovalent association with *E. coli* dihydrofolate reductase (eDHFR), a coumarinyl photocaging group, and a photocleavable 6-nitroveratryloxycarbonyl (Nvoc) moiety (Figure 1 A and the Supporting Information, Scheme S2). The coumarinyl group and Nvoc group are orthogonal photocaging groups that can be independently cleaved using light of different wavelengths[11] (Supporting Information, Scheme S3 and Figure S1). It is also possible to cleave the coumarinyl group first (> 98 % cleavage) without affecting the Nvoc group (< 1 %) using a relatively lower dose of 405 nm light[12]

Figure 1. A) The chemical structure of CONC (left) and its symbol (right) used in this work. B) Scheme of the optical control using the psCID system. C) HeLa cells co-expressing mCherry-eDHFR (red) and HaloTag-EGFP-ActA (mitochondria, green) were treated with CONC (1.1 µM, 30 min) and were illuminated with increasing doses of blue light (458 nm, 0–17 J cm⁻²) to induce protein dimerization. The dimerization process was gradually reversed by applying increasing doses of violet light (405 nm, 2–32 J cm⁻²). 1 unit dose (405 nm) = 1 J cm⁻²; 1 unit dose (458 nm) = 17 J cm⁻². Scale bar = 10 µm. D) Representative images of the mCherry-eDHFR (red) before PA, after PA (458 nm, I = 17 J cm⁻²), and after PD (405 nm, I = 32 J cm⁻²). The box shows images of HaloTag-EGFP-ActA (green). E) PCC analysis of the colocalization between mCherry-eDHFR and HaloTag-EGFP-ActA. Error bars = s.d. (n = 10); ****: $P < 0.0001$, Student's t-Test.

and subsequently cleave the Nvoc moiety using a higher dose of 405 nm light illumination.[6,7] Therefore, we speculate that the photocaging group and the photocleavable group could be controlled by 458 nm and 405 nm laser lines, respectively, or by a 405 nm laser line with different doses.

We first characterized if CONC can be used to reversibly control protein translocation in live cells by using light of different wavelengths (405 nm and 458 nm) (Figure 1 B). In HeLa cells, HaloTag-EGFP-ActA containing a C-terminal mitochondrial localization sequence from *Listeria monocytogenes protein ActA* was localized to mitochondria, while mCherry-eDHFR distributed throughout the cell. CONC was pre-localized to mitochondria through covalent binding to HaloTag. Subsequently, increasing doses of illumination at 458 nm (0–17 J cm⁻²) were used to induce stepwise targeting of mCherry-eDHFR to mitochondria. Afterwards, the dimerization was gradually reversed by raising the dose of illumination at 405 nm (2–32 J cm⁻²) (Figure 1 C,D). Pearson's correlation coefficient (PCC) analysis of the colocalization between mCherry-eDHFR and HaloTag-EGFP-ActA suggested that the dimerization is reversibly fine-tuned with light of two wavelengths (Figure 1 E). We also showed that the partial dimerization using less than 1 dose unit of 458 nm light can be reversed by 405 nm light (Supporting Information, Figure S2).

We envision that if both photoactivation (PA) and photo-deactivation (PD) can be achieved using light of a single wavelength (405 nm), an additional channel (cyan channel) can be saved for multi-color imaging. mCherry-eDHFR was readily targeted to mitochondria at lower doses of illumination (0–1 J cm⁻²), while the reverse process was achieved at higher doses of illumination (2–32 J cm⁻²; Supporting Information, Figure S3). Notably, both the dimerization degree and the dedimerization degree can be quantitatively controlled by applying different doses of light illumination. Therefore, these results demonstrate that this psCID system allows tunable and reversible control of protein dimerization in living cells by using light of a single wavelength (405 nm).

Next, we determined the dimerization and dedimerization rates of the psCID system in living cells. We locally photo-activate and photodeactivate a small region (indicated by a triangle) in HeLa cells to induce recruitment and dissociation of mCherry-eDHFR at the region of photoactivation (ROP) (Figure 2 A). We observed a rapid protein dimerization rate of $t_{1/2}$ (on) = 0.51 ± 0.02 s upon PA and an even faster dedimerization rate of $t_{1/2}$ (off) = 0.15 ± 0.03 s upon PD (Figure 2 B and Movie S1). We performed reversible targeting to a single mitochondrion (diameter < 1 µm) in the cell using the psCID system (Supporting Information, Figure S4). Therefore, very high spatial and temporal precision in live cells can be achieved using the psCID approach. We also performed global PA followed by local PD to highlight the versatility of the psCID system (Supporting Information, Figure S5).

We then demonstrated the control of intracellular cargo transport. BicD is a motor adaptor that recruits cytoplasmic dynein–dynactin complex to cargos (for example, vesicles and lipid droplets) and regulates dynein-dependent cargo transport. The N-terminal part of BicD is responsible for recruiting dynein and dynactin, while the C-terminal domain is required for tethering with specific cargos[13] (Supporting Information, Figure S6). We replaced the C-terminal domain of BicD2 with the eDHFR module and introduced HaloTag to Rab5a that
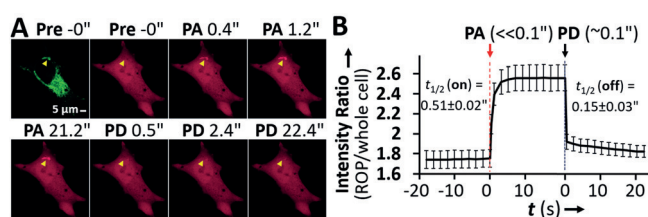
Figure 2. A) HeLa cells co-expressing Halo-EGFP-ActA (mitochondria, green) and mCherry-eDHFR (cytosol, red) were treated with CONC (1.1 µM, 30 min). A small region of photoactivation (ROP; indicated by the yellow triangle) in which a small cluster of mitochondria locates was illuminated by lower dose of 405 nm light (PA, 1 J cm⁻²) which leads to rapid local recruitment of mCherry-eDHFR to the ROP. Then a higher dose of 405 nm light (PD, 12 J cm⁻²) was applied to the same region, which leads to rapid dissociation of mCherry-eDHFR from the ROP. Scale bar = 5 µm. B) Time-course of protein translocation. The ratio of mCherry fluorescence intensity at the ROP versus that over the entire cell was plotted against time. Data were fit to a single exponential function to obtain the light-induced dimerization rate, $t_{1/2}$ (on) = 0.51 ± 0.02 s, and the dedimerization rate, $t_{1/2}$ (off) = 0.15 ± 0.03 s. Mean $\pm$ S.E.M. (n = 13).

specifically localizes to early endosomes (EEs). Hence, the tethering between BicD2 and cargo could be controlled by the psCID system (Supporting Information, Figure S6B).

We employed the N-terminal portion (1–594) of BicD2 (BicD2N). BicD2N-Citrine-eDHFR largely localized in the cytosol, while mCherry-HaloTag-Rab5a was localized at vesicular structures representing EEs (Figure 3B, frames 1 and 2). Upon PA, BicD2N was recruited to EEs along with the movement of EEs to the microtubule-organizing center (MTOC) at the cell center[14] (Figure 3B, frames 3 and 4).

Immediately after PD, BicD2N rapidly diffused to the entire cell, while EEs remained at MTOC (Figure 3B, frames 5 and 6; Figure 3C,G and Movie S2).

We analyzed the transport of an individual EE at the cell periphery (Figure 3B, the boxed region in the mCherry channel). This vesicle showed non-directional movement before PA (Figure 3D, frames −3 to −1; Figure 3F), and moved toward MTOC after PA (Figure 3D, frames 1–10). The directional transport of the vesicle was interrupted upon PD (Figure 3D, frames 11–13; Figure 3F). Accordingly, BicD2N was recruited to the vesicle upon PA and dissociated from the vesicle upon PD (Figure 3E). The trajectory of the vesicle showed that it is retrogradely transported for 10.1 μm in 245 s after PA with an average velocity of 41 nm s^{-1} (Figure 3F). These results suggest that the directional transport of vesicle resulted from the activation of dynein motors through the artificial tethering of the adaptor protein BicD2N to the cargo. Therefore, the cargo can be precisely positioned within the cell using the psCID approach.

We have used a modular design for the psCID system. CONC features two binding modules and two orthogonal photolabile moieties. The covalent binding of chlorhexyl moiety with HaloTag enables immobilization of the dimerizer to the protein that anchors at a specific cellular compartment, thereby suppressing the free diffusion of the dimerizer. The spatial resolution of the perturbation could then be achieved. Such a modular design enables enormous versatility of the system. For example, other binding modules could be used, such as SNAP tag, PYP tag, and FKBP tag.[15] Hence, a combination of orthogonal psCID systems would be useful for multiple layers of perturbation. The current psCID system uses blue light, which is limited in tissue penetration. However, it is also possible to use other photolabile moieties, such as two-photon caging groups,[16] which would shift the PA and PD light to longer wavelengths thus facilitating chemo-optogenetic control in living organisms.

The psCID approach can be a valuable complement for traditional optogenetic systems.[1c,d] First, the degree of dimerization and dedimerization is fine-tuned by the dose of illumination. Therefore, the number of molecules in the on/off state can be quantitatively controlled. This is very useful to emulate cellular states that are controlled by the
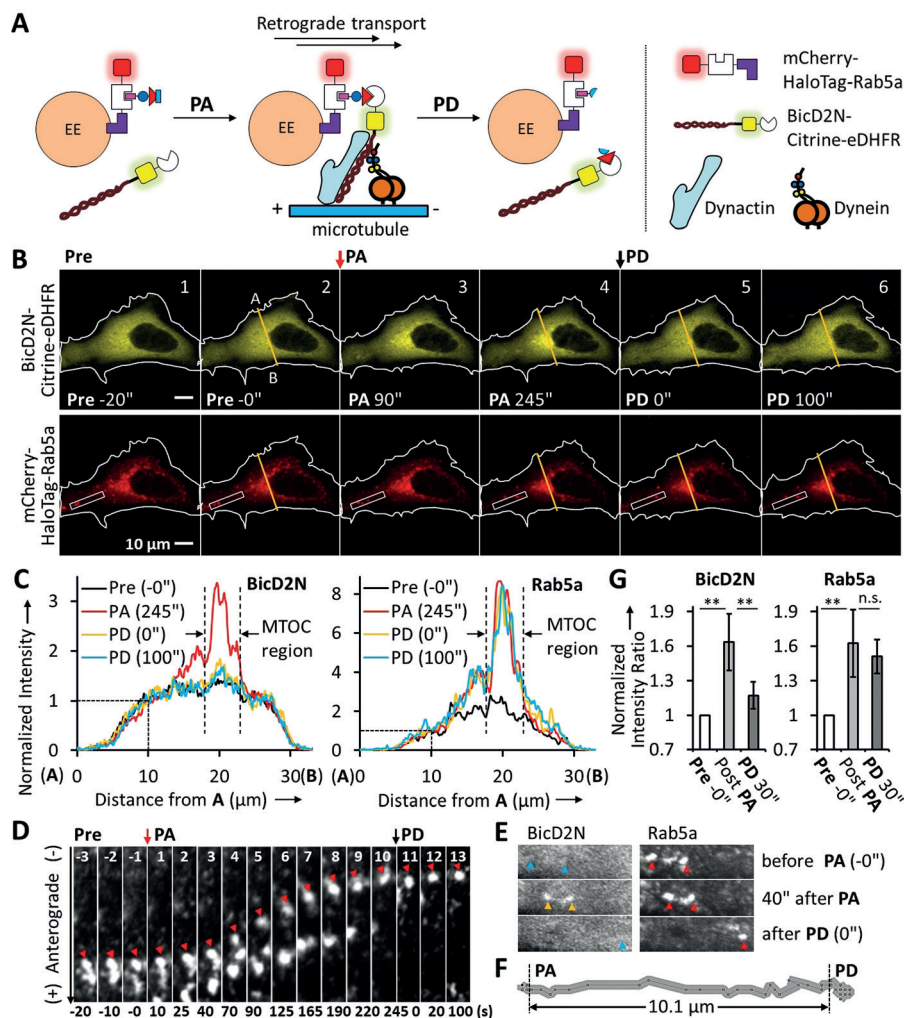
Figure 3. A) Scheme of the optical control using the psCID system. B) HeLa cells co-expressing BicD2N-Citrine-eDHFR and mCherry-HaloTag-Rab5a were treated with CONC (1.1 μM, 30 min). Before PA (frames 1 and 2), BicD2N was largely in the cytosol (upper panel) while mCherry-HaloTag-Rab5a was located to early endosomes (lower panel). After PA (405 nm), BicD2N-Citrine-eDHFR was recruited to EEs, along with the transport of EEs to MTOC (frames 3 and 4). After PD, BicD2N-Citrine-eDHFR rapidly diffused away to the entire cell, whereas EEs remained at the cell center (frames 5 and 6). Scale bar = 10 μm. C) The plotted line profiles, the orange lines in (B), of the Citrine and mCherry channels before PA (Pre −0″, black line), 254 s after PA (PA 245″, red line), immediately after PD (PD 0″, yellow line) and 100 s after PD (PD 100″, blue line). D) A single EE (indicated by the red triangle) at the cell periphery was tracked (the white box in (B)). The vesicle was almost steady before PA and was transported toward the cell center after PA. Its transport was disrupted after PD. E) BicD2N was recruited to individual EEs after PA and was immediately dissociated after PD. F) The trajectory of the EE shown in (D) before PA, after PA, and after PD (10 s interval). See also Movie S2. G) Statistical analysis (n = 6) of the fluorescence intensity ratio at the MTOC region versus that in the entire cell for both BicD2N (left) and Rab5a (right) just before PA (PA −0″), 2–3 min after PA while just before PD (Post PA), and 30 s after PD (PD 30″); **: P < 0.01, n.s.: not significant, Student's t-Test.

concentrations of the active protein. However, optogenetic systems using photosensitive proteins are mostly not readily tuned by light intensity, as photosensitive proteins exist in an equilibrium between active and inactive conformations. For the PhyB-PIF system, constant illumination with a ratio of stimulatory light and inhibitory light could be used to keep activation at a certain level. However, this is experimentally very challenging.[17] Second, this psCID system can be operated by a single short pulse (ms) of light. The PhyB-PIF system requires constant illumination to keep their on or off state.[2a] Some variants of the light-oxygen-voltage (LOV) domain can be operated by pulses of light in intervals of a few minutes.[18] Third, in contrast to many photosensitive proteins that suffer from non-zero affinity ($K_d = 1->100$ μM) in the off state and low affinity ($K_d = 0.1–10$ μM) in the on state, there is no binding between the caged dimerizer and the eDHFR module, while the decaged dimerizer binds to eDHFR in high affinity ($K_d = 1$ nM).[3a, 7] Hence, the dynamic range in chemo-optogenetic perturbation is significantly improved. Fourth, as shown in this work, optical perturbation at 405 nm using the psCID system can be combined with multi-color imaging, including mTurquoise2 (excitation at 458 nm), Citrine (514 nm), mCherry (561 nm), and Atto740 dye (750 nm), which would be limited using photosensitive proteins owing to the overlap of absorption spectra (for example, LOV, 400–500 nm; Cry2, 390–500 nm; PhyB, 550–800 nm; and Dronpa, 350–530 nm). One limitation of the current psCID system is that it allows only one round of reversible control by light.

The psCID system is reversible, tunable, and acute with high spatial resolution at micrometer scale. Both photo-activation and photodeactivation are very rapid with $t_{1/2}$ (on/off) = 0.1–0.5 s. The turn-on/off speed is orders of magnitude faster than current optogenetic systems,[9] which is highly valuable for studying fast biological processes. We envision that the psCID approach could open a new avenue for spatiotemporal control of protein or cargo distribution, which could be highly valuable for investigating a wide range of dynamic cellular processes.

[1] a) R. DeRose, T. Miyamoto, T. Inoue, *Pflug. Arch. Eur. J. Phys.* **2013**, *465*, 409–417; b) S. Voss, L. Klewer, Y. W. Wu, *Curr. Opin. Chem. Biol.* **2015**, *28*, 194–201; c) D. Tischer, O. D. Weiner, *Nat. Rev. Mol. Cell Biol.* **2014**, *15*, 551–558; d) M. Weitzman, K. M. Hahn, *Curr. Opin. Cell Biol.* **2014**, *30*, 112–120; e) M. Putyrski, C. Schultz, *FEBS Lett.* **2012**, *586*, 2097–2105.

[2] a) A. Levskaya, O. D. Weiner, W. A. Lim, C. A. Voigt, *Nature* **2009**, *461*, 997–1001; b) J. Niu, M. B. Johny, I. E. Dick, T. Inoue, *Biophys. J.* **2016**, *111*, 1132–1140; c) M. Yazawa, A. M. Sadaghiani, B. Hsueh, R. E. Dolmetsch, *Nat. Biotechnol.* **2009**, *27*, 941–U105; d) Y. I. Wu, D. Frey, O. I. Lungu, A. Jaehrig, I. Schlichting, B. Kuhlman, K. M. Hahn, *Nature* **2009**, *461*, 104–108; e) M. J. Kennedy, R. M. Hughes, L. A. Peteya, J. W. Schwartz, M. D. Ehlers, C. L. Tucker, *Nat. Methods* **2010**, *7*, 973–975.

[3] a) P. Liu, A. Calderon, G. Konstantinidis, J. Hou, S. Voss, X. Chen, F. Li, S. Banerjee, J. E. Hoffmann, C. Theiss, L. Dehmelt, Y. W. Wu, *Angew. Chem. Int. Ed.* **2014**, *53*, 10049–10055; *Angew. Chem.* **2014**, *126*, 10213–10219; b) S. H. Feng, V. Laketa, F. Stein, A. Rutkowska, A. MacNamara, S. Depner, U. Klingmuller, J. Saez-Rodriguez, C. Schultz, *Angew. Chem. Int. Ed.* **2014**, *53*, 6720–6723; *Angew. Chem.* **2014**, *126*, 6838–6841; c) Y. C. Lin, Y. Nihongaki, T. Y. Liu, S. Razavi, M. Sato, T. Inoue, *Angew. Chem. Int. Ed.* **2013**, *52*, 6450–6454; *Angew. Chem.* **2013**, *125*, 6578–6582.

[4] a) N. Umeda, T. Ueno, C. Pohlmeyer, T. Nagano, T. Inoue, *J. Am. Chem. Soc.* **2011**, *133*, 12–14; b) A. V. Karginov, Y. Zou, D. Shirvanyants, P. Kota, N. V. Dokholyan, D. D. Young, K. M. Hahn, A. Deiters, *J. Am. Chem. Soc.* **2011**, *133*, 420–423.

[5] M. Zimmermann, R. Cal, E. Janett, V. Hoffmann, C. G. Bochet, E. Constable, F. Beaufils, M. P. Wymann, *Angew. Chem. Int. Ed.* **2014**, *53*, 4717–4720; *Angew. Chem.* **2014**, *126*, 4808–4812.

[6] E. R. Ballister, C. Aonbangkhen, A. M. Mayo, M. A. Lampson, D. M. Chenoweth, *Nat. Commun.* **2014**, *5*, 5475.

[7] X. Chen, M. Venkatachalapathy, D. Kamps, S. Weigel, R. Kumar, M. Orlich, R. Garrecht, M. Hirtz, C. M. Niemeyer, Y. W. Wu, L. Dehmelt, *Angew. Chem. Int. Ed.* **2017**, *56*, 5916–5920; *Angew. Chem.* **2017**, *129*, 6010–6014.

[8] W. O. Hancock, *Nat. Rev. Mol. Cell Biol.* **2014**, *15*, 615–628.

[9] P. van Bergeijk, C. C. Hoogenraad, L. C. Kapitein, *Trends Cell Biol.* **2016**, *26*, 121–134.

[10] C. C. Hoogenraad, A. Akhmanova, *Trends Cell Biol.* **2016**, *26*, 327–340.

[11] V. San Miguel, C. G. Bochet, A. del Campo, *J. Am. Chem. Soc.* **2011**, *133*, 5380–5388.

[12] V. Hagen, J. Bendig, S. Frings, T. Eckardt, S. Helm, D. Reuter, U. B. Kaupp, *Angew. Chem. Int. Ed.* **2001**, *40*, 1045–1048; *Angew. Chem.* **2001**, *113*, 1077–1080.

[13] R. J. McKenney, W. Huynh, M. E. Tanenbaum, G. Bhabha, R. D. Vale, *Science* **2014**, *345*, 337–341.

[14] M. Bentley, H. Decker, J. Luisi, G. Banker, *J. Cell Biol.* **2015**, *208*, 273–281.

[15] X. Chen, Y. W. Wu, *Org. Biomol. Chem.* **2016**, *14*, 5417–5439.

[16] N. Ankenbruck, T. Courtney, Y. Naro, A. Deiters, *Angew. Chem. Int. Ed.* **2018**, *57*, 2768–2798; *Angew. Chem.* **2018**, *130*, 2816–2848.

[17] J. E. Toettcher, O. D. Weiner, W. A. Lim, *Cell* **2013**, *155*, 1422–1434.

[18] H. Wang, M. Vilela, A. Winkler, M. Tarnawski, I. Schlichting, H. Yumerefendi, B. Kuhlman, R. Liu, G. Danuser, K. M. Hahn, *Nat. Methods* **2016**, *13*, 755–758.